

Siphonophore Phylogeny

Catriona Munro^{1*}, Stefan Siebert^{1,2*}, Felipe Zapata^{1,3}, Mark Howison⁴, Alejandro Damian Serrano^{1,9}, Samuel H Church^{1,5}, Freya Goetz^{1,6}, Phil Pugh⁷, Steven H.D. Haddock⁸, Casey W. Dunn^{1,9**}

¹ Department of Ecology and Evolutionary Biology, Brown University, Providence, RI 02912, USA

² Current address: Department of Molecular & Cellular Biology, University of California at Davis, Davis, CA 95616, USA

³ Current address: Department of Ecology and Evolutionary Biology, University of California Los Angeles, Los Angeles, CA 90095, USA

⁴ Brown Data Science Practice, Brown University, Brown University, Providence, RI 02912, USA

⁵ Department of Organismic and Evolutionary Biology, Harvard University, Cambridge, MA 02138, USA

⁶ Current address: Smithsonian Institution, National Museum of Natural History, Washington, DC 20560, USA

⁷ National Oceanography Centre, Southampton, SO14 3ZH, UK

⁸ Monterey Bay Aquarium Research Institute, Moss Landing, CA 95039, USA

⁹ Current address: Department of Ecology and Evolutionary Biology, Yale University, New Haven, CT 06520, USA

* Authors contributed equally

** Corresponding author, casey.dunn@yale.edu

Abstract

Introduction

Siphonophores are a group of 188 valid species within Hydrozoa (Cnidaria), the vast majority of which are members of the plankton (fig. 1). Siphonophores are colonial, and are composed of zooids that are each homologous to solitary animals, but are physiologically integrated (Totton and Bargmann, 1965; Mackie et al., 1988; Dunn and Wagner, 2006). Siphonophores differ significantly from all other colonial hydrozoans in terms of colony structure, development, and the degree to which they are functionally specialized (Beklemishev, 1969; Cartwright and Nawrocki, 2010). A siphonophore colony arises from a single embryo, which forms a protozooid and a growth zone from which other genetically identical zooids bud asexually (Carré, 1967, 1969; Carré and Carré, 1991, 1995). Each zooid is generated asexually, arises in the same repeating species-specific pattern, and is functionally specialized for a particular task (e.g feeding, reproducing, swimming) (fig. 2) (Dunn and Wagner, 2006). Siphonophores are found at all depths - most species are planktonic, with the exception of one pleustonic species (*Physalia physalis*, Portuguese man of war) that lives at the interface of water and air, and a small clade of benthic siphonophores, the Rhodaliidae (Totton, 1960; Pugh, 1983; Carré and Carré, 1995). They are among the most abundant gelatinous predators in the open ocean, and play an important ecological role in oceanic waters (Williams and Conway, 1981; Purcell, 1981; Pugh, 1984; Pugh et al., 1997; Pagès et al., 2001).

Siphonophores are monophyletic and nested within the Hydrodolina, although relationships among the major lineages of the Hydrodolina remain difficult to resolve (Cartwright et al., 2008; Cartwright and Nawrocki, 2010; Zapata et al., 2015). The most resolved siphonophore phylogeny to date focused on two genes (16S, 18S) from 52 siphonophore taxa, and resolved many long standing questions about siphonophore biology, including the relationships of the three historically recognised groups (Cystonectae, Physonectae, and Calycophorae) (Dunn et al., 2005). The cystonects were found to be sister to all other siphonophores, while the calycophorans were nested within physonects (the name Codonophora was given to this clade)(Dunn et al., 2005).

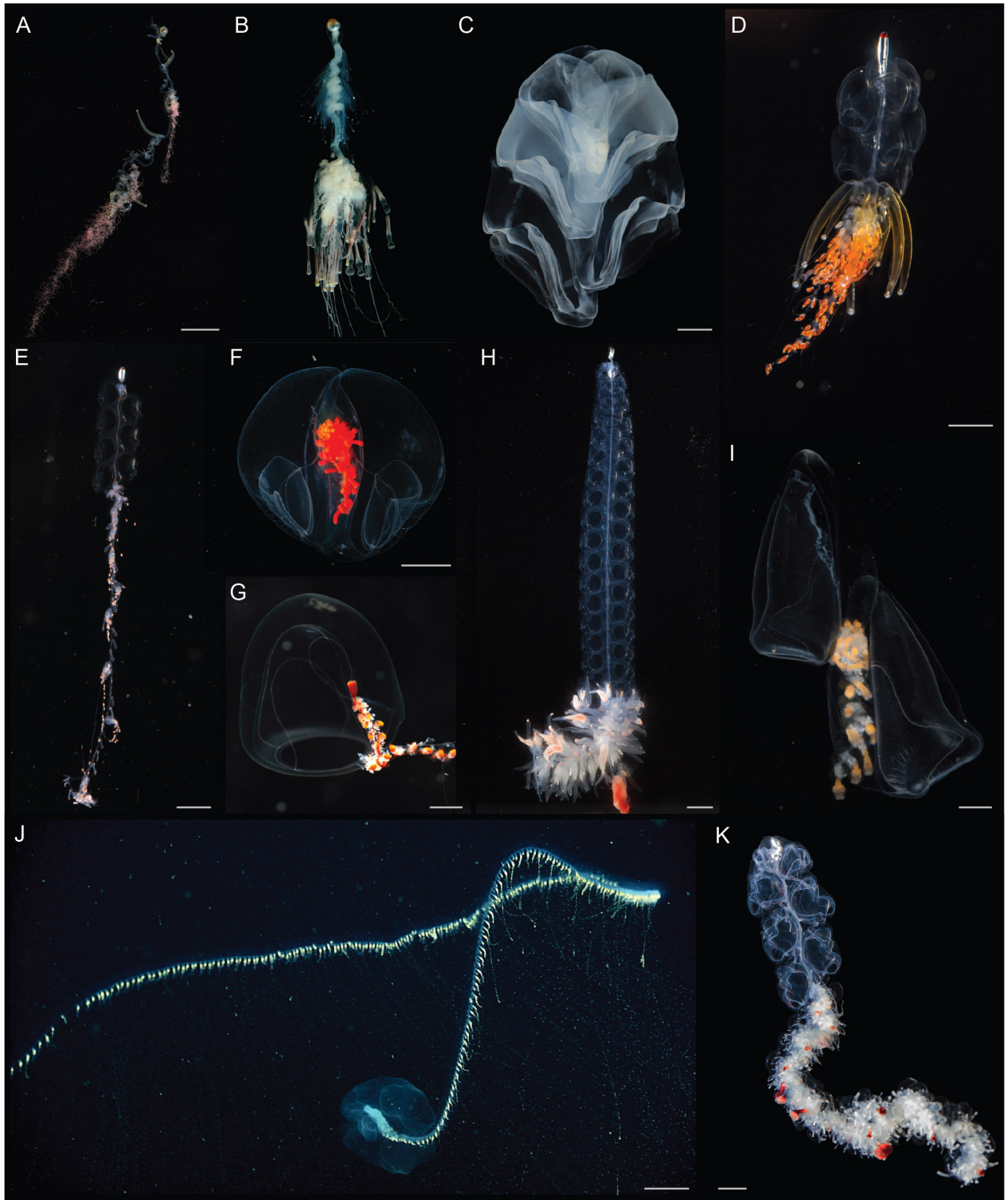


Figure 1: Photographs of representatives of the major groups of siphonophores. (A) *Rhisophysa eysenhardtii*, scale bar = 1 cm. (B) *Bathypysa conifera*, scale bar = XXX. (C) *Hippopodius hippopus*, scale bar = 5 mm. (D) *Physophora hydrostatica*, scale bar = 5 mm. (E) *Nanomia bijuga*, scale bar = 1 cm. (F) *Desmophyses haematogaster*, scale bar = 5 mm. (G) *Sphaeronectes christiansonae*, scale bar = 2 mm. (H) *Lychnagalma utricularia*, scale bar = 1 cm. (I) *Kephyes hiulcus*, scale bar = 2 mm. (J) *Praya dubia*, scale bar = 4 cm . (K) *Apolemia* sp., scale bar = 1 cm.

The Apolemiidae are sister to all other Codonophora, however there was little resolution of deep relationships within Codonophora. The history of colony structure and budding was investigated by mapping these traits to the tree, and suggesting a complex history of zooid gain and loss. Resolving deep relationships within Codonophora is key to resolving the evolution of several character traits, including sexual systems (monoecy vesus dioecy) or the gain and loss of particular zooids, such as palpons.

Siphonophores are difficult to collect, in part because they are fragile (nets destroy all but the most robust parts of the colony), but also because many species are found in the deep sea (Youngbluth, 1984; Dunn et al., 2005). Specimen sampling for the previous phylogeny, and this new work, is enabled by modern collection techniques, including blue-water scuba diving and remotely operated vehicles (ROVs). Here we present a broadly sampled phylogenomic analysis of Siphonophora, assessing transcriptomic data from 34 siphonophore species and 9 outgroup species. Using 1071 genes shared across species, we are able to resolve deep relationships within the siphonophore phylogeny and reconstruct the evolutionary history of characters, including zooid type, life history traits, and habitat.

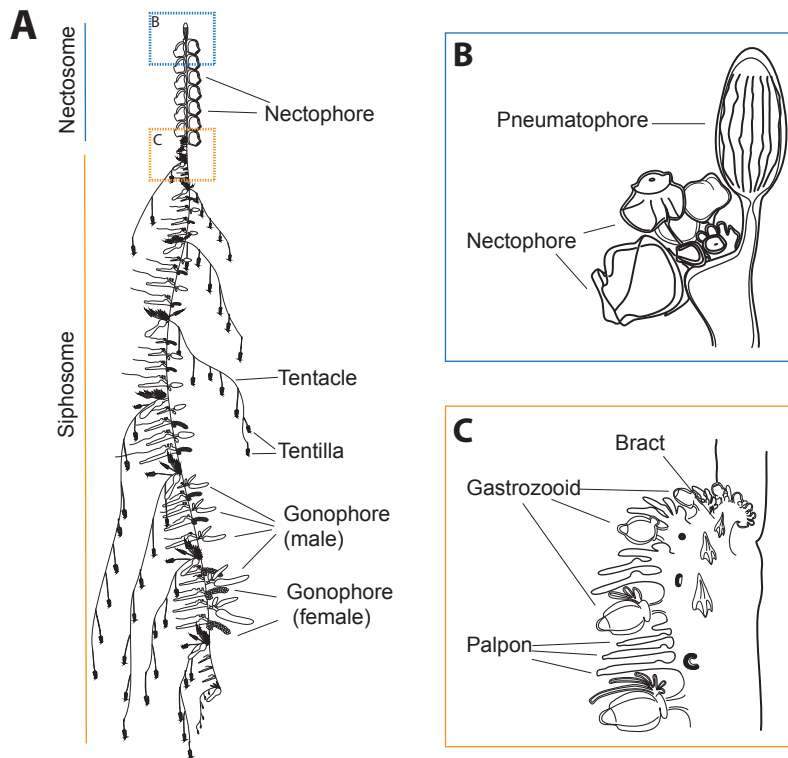


Figure 2: Schematic of the siphonophore *Nanomia bijuga*, oriented with the anterior of the colony at the top, and the ventral side to the left. Adapted from http://commons.wikimedia.org/wiki/File:Nanomia_bijuga_whole_animal_and_growth_zones.svg, drawn by Freya Goetz. (A) Overview of the whole mature colony. (B) Inset of the nectosomal growth zone with pneumatophore. A series of buds gives rise to nectophores. (C) Inset of the siphosomal growth zone. Probuds subdivide to give rise to zooids in repeating-units (cormidia). Cormidial boundaries are marked by a gastrozooid.

Methods

This manuscript is an executable document computed directly from the data, providing an explicit and reproducible description of all findings. All scripts for the analyses are available in a git repository at

https://github.com/caseywdunn/siphonophore_phylogeny_2017. The most recent commit at the time of the analysis presented here was b5c57eb5f980051b2abfe8e36998ff76d1a0e082.

Collecting

Collection data on all examined specimens, a description of the tissue that was sampled from the colony, collection mode, sample processing details, mRNA extraction methods, sequencing library preparation methods and sequencing details are summarized in supplementary table 1. Monterey Bay and Gulf of California specimens were collected by remotely operated underwater vehicle (ROV) or during blue-water scuba dives. *Chelophyses appendiculata* and *Hippopodius hippopus* specimens were collected in the bay of Villefranche-sur-Mer, France, during a plankton trawl on 04/13/11. Available physical vouchers have been deposited at the Museum of Comparative Zoology (Harvard University), Cambridge, MA, or had been previously deposited at the United States National Museum (Smithsonian Institution), Washington, DC. Accession numbers are given in supplementary table X. In cases where physical vouchers were unavailable we provide photographs to document species identity (table x).

Sequencing

When possible specimens were starved overnight in filtered seawater at temperatures close to ambient water temperatures at the time point of specimen collection (supplementary table x). mRNA was extracted directly from tissue using a variety of methods (supplementary table x): Magnetic mRNA Isolation Kit (NEB, #S1550S), Invitrogen Dynabeads mRNA Direct Kit (Ambion, #61011), Zymo Quick RNA MicroPrep (Zymo #R1050), or from total RNA after Trizol (Ambion, #15596026) extraction and through purification using Dynabeads mRNA Purification Kit (Ambion, #61006)- in case of anticipated very small total RNA quantities, only a single round of bead purification was performed; or Trizol directly into the Illumina TruSeq Stranded Library Kit. Extractions were performed according to the manufacturer's instruction. Any resulting higher rRNA read counts were dealt with further downstream in the bioinformatics workflow. Libraries were prepared for sequencing using the Illumina TruSeq RNA Sample Prep Kit (Illumina, #FC-122-1001, #FC-122-1002), the Illumina TruSeq Stranded Library Prep Kit (Illumina, #RS-122-2101) or the NEBNext RNA Sample Prep Master Mix Set (NEB, #E6110S). We collected long read paired end Illumina data for *de novo* transcriptome assembly. In the case of large tissue inputs, libraries were sequenced separately for each tissue, subsequently subsampled and pooled *in silico*. Libraries were sequenced on the HiSeq 2000, 2500, and 3000 sequencing platforms (supplementary table x).

Analysis

New data were analysed in conjunction with 13 publically available datasets, with a total number of 43 species. Sequence assembly, annotation, Maximum Likelihood (ML) phylogenetic analysis were conducted with the tool Agalma (Dunn et al., 2013), v. 1.00, and Bayesian Inference (BI) analyses were conducted using Phylobayes(Lartillot et al., 2009) v. 1.7a-mpi. Source code for all analysis steps, sequence alignments, sampled and consensus trees, and voucher information are available in a git repository https://github.com/caseywdunn/siphonophore_phylogeny_2017.

Two outgroup species, *Atolla vanhooffeni* and *Aegina citrea*, were removed from the final supermatrix and phylogeny due to low gene occupancy (gene sampling of 20.8% and 14.5% respectively in a 50% occupancy matrix with 2,203 genes). ML analyses were conducted on the unpartitioned supermatrix using the WAG+Γ model of amino acid substitution, and bootstrap values were estimated using 1000 replicates. BI was conducted using two different CAT models, CAT-Poisson and CAT-GTR (Lartillot and Philippe, 2004). Two independent MCMC chains were run under the CAT-GTR model, and four independent MCMC chains were run under the CAT-Poisson model. The CAT-GTR and CAT-poisson models did not converge after a long CPU time, and only the results from the CAT-poisson model are included here.

Morphological character data used in trait mapping were obtained from the literature, or from direct observation of available voucher material. We used stochastic character mapping to infer the probable

evolution of traits on the tree in R using the `phytools` package (Revell, 2012, Huelsenbeck et al. (2003)). Subsequent analyses were conducted in R and integrated into this manuscript with the `knitr` package. See Supplementary Information for R package version numbers.

Hypothesis testing

We used the Swofford-Olsen-Waddell-Hillis (SOWH) test (Swofford et al., 1996) to evaluate two hypotheses: (i) physonects are monophyletic (Totton and Bargmann, 1965); (ii) monoecious species are monophyletic (Dunn et al., 2005). As the sexual system of *Rudjakovia sp* is unclear, we carried out two tests of the monophyly of monoecy, one with *Rudjakovia sp* included as a monoecious species, and one without. We used SOWHAT (Church et al., 2015) dev. version 0.39 (commit fd68ef5733c095c7000a4f92dc8c0daaddeec3b9) to carry out the SOWH tests in parallel with the default options and an initial sample size of 100 (source code can be found in the git repository). For each hypothesis we defined a topology with a single constrained node that was inconsistent with the most likely topology (figure 3 x). We used a threshold for significance of 0.05 and following the initial 100 samples, we evaluated the confidence interval around the p-value to determine if more samples were necessary.

Results and Discussion

Species phylogeny and hypothesis testing

Specimens were collected in the eastern Pacific Ocean, Mediterranean, and the Gulf of California (table 1). All sequence data have been deposited in the sequence read archive (SRA). The analyses presented here consider 34 siphonophore species and 9 outgroup species. This includes new data for 30 species. Summary statistics for expression libaries are given in supplementary table x. In the final analyses, we sampled 1,071 genes to generate a supermatrix with 60% occupancy and a length of 378,468 amino acids (gene occupancy matrix - supplementary figure 1).

Maximum likelihood analyses had 1000 replicates. We ran 4 phylobayes chains, and visual inspection of the traces indicated that a burn in of 400 trees was sufficient for all runs. This left 15847 trees in the posterior. The phylobayes chains did not converge after a long CPU time, and uncertainty remains around the placement of *Erenna richardi*, and also *Nanomia bijuga*. Within the ML analysis, the placement of *Erenna richardi* is also unstable. Alternative topologies for these nodes are shown in figure 3 x.

pdf
2

These findings are largely consistent with a previous analysis based on two genes (16S and 18S ribosomal RNA) (Dunn et al., 2005). Cystonectae is the sister group to the remaining siphonophores, Calycophorae is nested within the paraphyletic “Physonectae”, and *Apolemia* is sister to all other Codonophora. In addition, multiple nodes that were not resolved in the previous two-gene analysis do receive strong support in this 1,071-gene transcriptome analysis. *Physophora gilmeri*, along with *Lychnagalma utricularia* (not included in previous phylogeny) are sister to the Agalmatidae *sensu stricto*. *Craseoa lathetica* and *Desmophyses haematogaster* are sister to *Hippopodius hippopus*. *Cordagalma cordiforme* was previously unresolved, while in this analysis *Cordagalma sp* falls within the Agalmatidae. Additionally, there is strong support for *Bargmannia* as sister to all non-Apolemid codonophorans.

We tested the following three alternative phylogenetic hypotheses against the most likely tree topology: (i) physonect siphonophores are monophyletic, (ii) monoecious siphonophores (not including *Rudjakova sp.*) are monophyletic, and (iii) monoecious siphonophores (including *Rudjakova sp.*) are monophyletic (figure 3 xx). In all three cases the alternative hypothesis was rejected (p-value <0.01, confidence interval: <0.001 - 0.03).

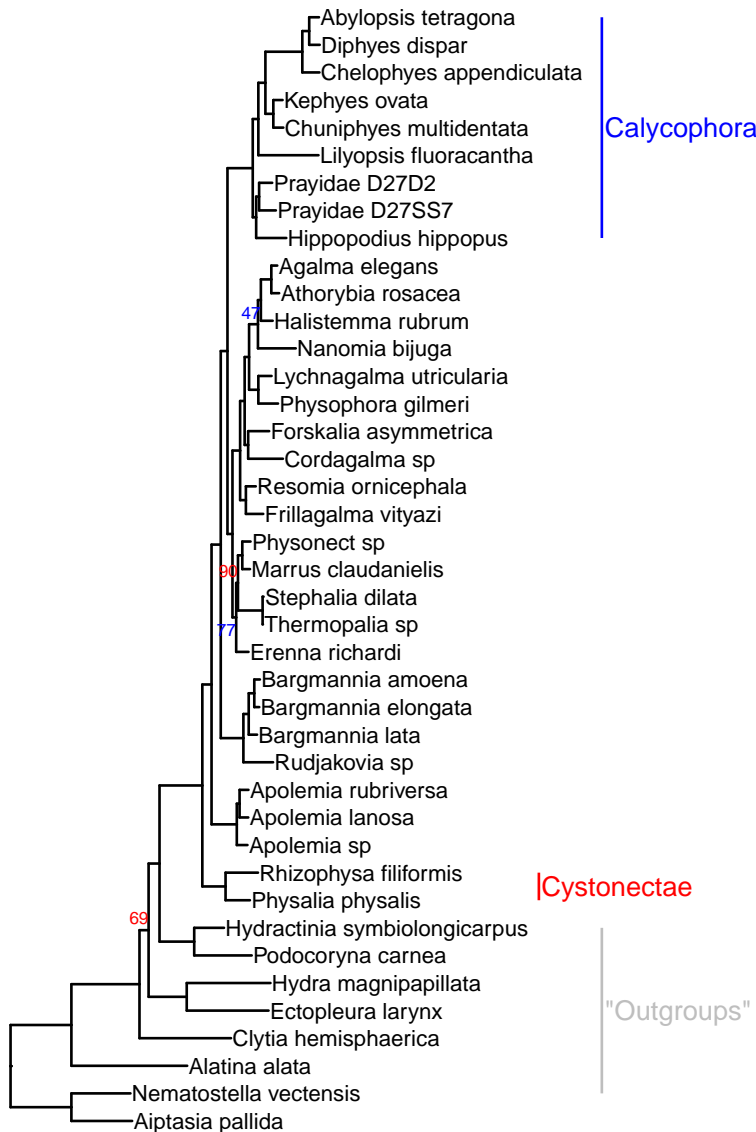


Figure 3: Phylogram of siphonophore relationships. Node labels indicate bootstrap support percent, unnumbered nodes have 100% support. The image was rendered with ggtree (Yu et al., 2016).

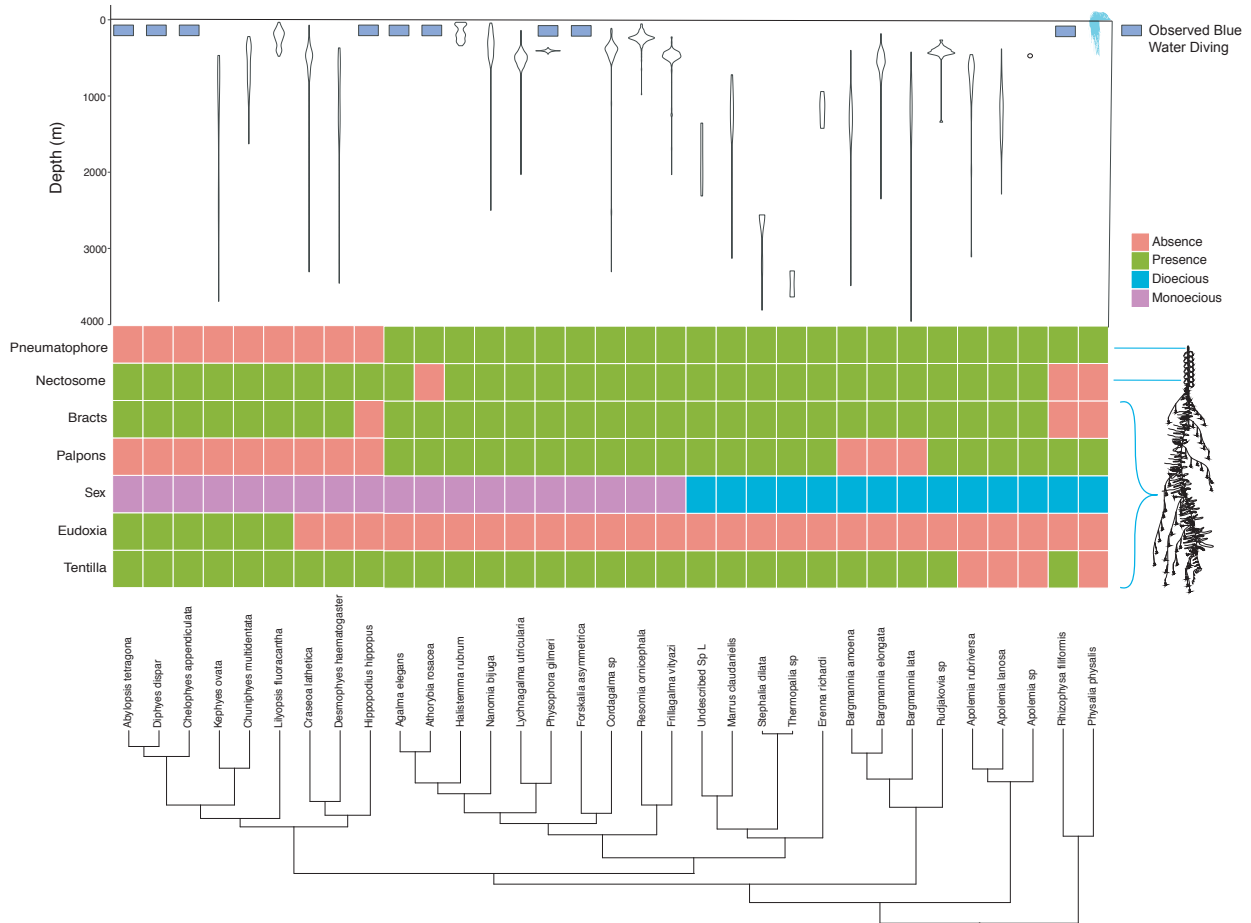


Figure 4: Siphonophore phylogeny showing the distribution of the main anatomical characters and the bathymetric distributions of the different species.

New data	Species	SRA Number	Depth (m)	Lat Lon
N	<i>Agalma elegans</i>		3-20	35.56 N 122.55 W
Y	<i>Bargmannia elongata</i>		412/805/636/818	36.12 N 122.67 W
Y	<i>Frillagalma vityazi</i>		407	36.69 N 122.05 W
Y&N	<i>Nanomia bijuga</i>		414/387	36.60 N 122.15 W
N	<i>Physalia physalis</i>	SRS431081		
N	<i>Abylopsis tetragona</i>	SRX288276		
N	<i>Aegina citrea</i>	SRS893439		
N	<i>Aiptasia pallida</i>	SRX231866		
N	<i>Alatina alata</i>	SRS893440		
Y	<i>Apolemia rubriversa</i>		767	36.70 N 122.05 W
N	<i>Atolla vanhoeffeni</i>	SRS893451		
Y	<i>Chelophyes appendiculata</i>		0-30	
Y	<i>Chuniphyes multidentata</i>		327	36.79 N 122.00 W
N	<i>Clytia hemisphaerica</i>			
Y	<i>Cordagalma sp</i>		252	36.70 N 122.06 W
N	<i>Ectopleura larynx</i>	SRX315375		
Y	<i>Erenna richardi</i>		1044	36.61 N 122.38 W
Y	<i>Forskalia asymmetrica</i>		253	36.80 N 122.00 W
Y	<i>Hippopodius hippopus</i>		0-30	43.69, 7.315
N	<i>Hydra magnipapillata</i>			
N	<i>Hydractinia symbiolongicarpus</i>	SRX474878		
Y	<i>Kephyses ovata</i>		452	36.36 N 122.81 W
Y	<i>Lilyopsis fluoracantha</i>		320	36.69 N 122.04 W
Y	<i>Lychnagalma utricularia</i>		431	36.69 N 122.04 W
Y	<i>Marrus claudanielis</i>		1427	36.07 N 122.29 W
N	<i>Nematostella vectensis</i>			
Y	<i>Physonect sp</i>		1463	36.70 N 122.57 W
Y	<i>Podocoryna carneaa</i>			
Y	<i>Prayidae D27SS7</i>		1363	35.48 N 123.64 W
N	<i>Prayidae D27D2</i>	SRX288432		
Y	<i>Resomia ornicephala</i>		322	35.48 N 123.86 W
Y	<i>Rhizophysa filiformis</i>		10	27.23 N 110.46 W
Y	<i>Stephalia dilata</i>		3074	35.62 N 122.67 W
Y	<i>Apolemia lanosa</i>		1073	36.70 N 122.08 W
Y	<i>Apolemia sp</i>		461	36.60 N 122.15 W
Y	<i>Bargmannia amoena</i>		1251	36.70 N 122.08 W
Y	<i>Bargmannia lata</i>		1158	36.067 N 122.30 W
Y	<i>Rudjakovia sp</i>		334	36.00 N 122.42 W
Y	<i>Thermopalia sp</i>		3255	36.39 N 122.67 W
Y	<i>Physophora gilmeri</i>		242	36.36 N 122.40 W
Y	<i>Halistemma rubrum</i>			24.68 N 109.90W
Y	<i>Athorybia rosacea</i>			22.92 N 108.36 W
Y	<i>Diphyes dispar</i>		0-30	35.93 N 122.93 W

Table 1: Table 1. A complete list of specimens collected for this work.

Character Evolution

In our previous siphonophore phylogenetic analysis (Dunn et al., 2005) there were several characters left with equivocal evolutionary histories, due to unresolved relationships between physonects. With our current cladistic resolution, we were able to answer some of the questions left open:

Evolution of Monoecy

[Citation needed] noticed for the first time that some siphonophores were monoecious and others were dioecious. Our analyses in 2005 reconstructed this character and found a great amount of phylogenetic conservatism, with an unambiguous resolution of the MRCA (most recent common ancestor) as dioecious, and the appearance of monoecy in several taxa and clades (including Calycophorae) within the polytomy. Figure 5a shows the evolution of sex distribution in siphonophores under the current better-resolved tree model, and it strongly indicates that monoecy in siphonophores from a dioecious ancestor occurred twice, in the branch leading to Calycophorae and in the branch leading to Agalmatids (*sensu lato*). There is a small probability for an alternative scenario featuring a single gain of monoecy before the split of Calycophorae, with a subsequent derived shift back to dioecy in the *Marrus-Erenna* clade.

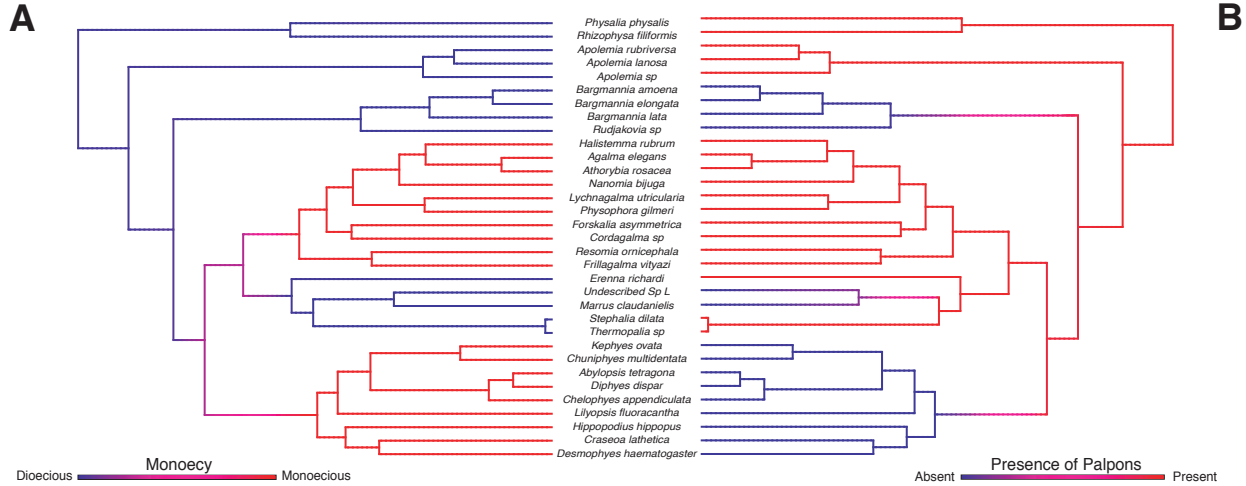


Figure 5: Figure 5. Stochastic mapping reconstruction of the evolutionary history of A) palpon zooids, and B) distribution of sexual zooids on the colonies.

The Evolution of Zooid Types

One of the most striking aspects of siphonophore biology is their diversity of unique zooid types. Other colonial cnidarians (such as Hydractinia) and some bryozoans (example) have been found to have up to X different zooid types [Citation1 , Citation 2]. The siphonophore genus *Forskalia* has 6 basic zooid types (pneumatophore, nectophore, gastrozooid, palpon, bract, and gonophore), and a total of 10 counting subtypes (4 types of bract, male & female gonophores). Diphyomorphs have more than 1 type of nectophore, while Cystonects have none. Here we reconstruct the evolutionary origins of the different zooid types on the present transcriptome tree.

Nectophores are retained modified medusae that Codonophora use for coordinated colony-level swimming. The nectosome is the region of the colony that develops from the nectosomal growth zone. Unlike the siphosomal growth zone, the nectosome does not bud gastrozooids, but nectophores (and in the case of *Apolemia*, also palpons). In fact, with the exception of *Physalia physalis* (which grows small nectophores near the gonodendra), siphonophore nectophores are exclusively found on the nectosome. It is possible that the MRCA of siphonophores had a nectosome, which has lost on the branch leading to Cystonects. We cannot exclude with certainty the alternative hypothesis of a nectosome-less ancestor followed by a gain of the nectosome in the branch leading to the Codonophora. The nectosome probably arose as a duplication of the siphosome, followed by functional specialization in propelling the colony. The nectosome has been lost within Codonophora in the genus *Athorybia*.

Following the colony development orientation framework presented in (citation), the nectosome can be located in a dorsal or a ventral position. Our ancestral reconstructions for this character (Supp figure) show that a ventrally-oriented nectosome was the ancestral form in siphonophores, and that a dorsal nectosome has evolved twice independently, in the branches leading to the Agalmatidae (sensu stricto) and the branch leading to the *Bargmannia* species.

All Codonophora (with the exception of *Athorybia* species) have a nectosome, but the number and subtypes of nectophores present varies greatly between species. As shown in Figure X, most Codonophora presents the ancestral nectosome with multiple nectophores of the same subtype. However, Calycophorans evolved a different system with just 2 nectophores of one type. This shift may be associated with the loss of the pneumatophore. Not all Calycophorans remained with this arrangement. The Hippopodidae returned to bearing multiple identical nectophores, many of which are inactive and serve functions of defense (like a shell to retract in) and buoyancy. As in the rest of Calycophorans, the Hippopodids only use 2 nectophores to propel the colony. Another interesting shift occurs in the branch leading to Diphyomorphs, where the 2

nectophores specialize into 2 subtypes, associated with a shift into a vertically aligned position and pointed bell shapes. The 2 types function together in a coupled hydrodynamic system that allows very fast escape responses (Mackie 1964).

Bracts are highly reduced zooids unique to siphonophores, but they are only present in the Codonophora. As with the nectosome, we have ambiguity determining whether the MRCA of siphonophores had bracts or not. The MRCA of Codonophora had only one bract subtype, which was lost in Hippopodidae, *Physophora hydrostatica* (however, they are present in its sister species, *P. gilmeri* included in the present phylogeny), and in *Gymnopraia lapislazula*. Bracts are functional for protection of the delicate zooids and to help maintain neutral buoyancy. Some calycophorans are able to actively exclude sulphate ions in their bracts to adjust their buoyancy along the colony (Bidigare & Biggs, 1980).

The ancestral siphonophore certainly had a pneumatophore, since both Cystonects and most Codonophorans possess one (Figure 4). This unique zooid fills itself with gas, which helps the colony float and maintain its orientation in the water column. Recent evidence of neural arrangement in the pneumatophore of *Nanomia bijuga* (Church, 2013) suggests it could also gather information on relative pressure changes (and thus depth changes), helping regulate geotaxis. Despite its multiple biological functions, it was lost in the Calycophorae and never gained again in that clade. Calycophorans rely on the ionic balance of their gelatinous nectophores and bracts to retain posture and neutral buoyancy.

Palpons are modified mouthless gastrozooids used for digestion and circulation of the gastrovascular fluid. They were present in the MRCA of siphonophores (Figure 5b), retained in most species, but lost three times independently in the branches leading to Pyrostephidae (represented here by the genera *Bargmannia* and *Rudjakovia*), in Calycophorans, and in *Marrus claudanielis*. These taxa might have found other avenues to effectively circulate nutrients across the colony.

The Gain and Loss of Tentilla

The most complex nematocyst batteries of Cnidaria can arguably be found among the siphonophores, hanging in regularly spaced tentacle side branches called tentilla. Most hydrozoans, including the clade that contains siphonophores, bear simple tentacles (tentacles with no side branches). It is still an open question whether the MRCA of Siphonophora had simple or branched tentacles. The only siphonophores genera regarded as lacking tentilla are *Physalia physalis* and *Apolemia* spp., and *Bathyphysa conifera*. Since *B. conifera* is the only member of the Rhizophysidae (and of the *Bathyphysa* genus) lacking tentilla, we can safely assume this is a case of secondary loss. When we reconstruct the evolution of this character on the current phylogeny, we find that 70% of simulations support an MRCA bearing tentilla, with two independent losses leading to *Physalia* and *Apolemia*. However, this leaves a 30% support for a simple-tentacled MRCA followed by 2 independent gains of tentilla in the branches leading to Rhizophysidae and {*Bargmannia*, *Diphyes*}.

A key issue here is how we code for absence of tentilla, especially for the case of *Physalia physalis*. The tentacles of this species, when uncoiled, show very prominent, evenly spaced, bulging buttons which contain on their ectoderm all active and functionally arranged nematocysts used by the organism for prey capture. Siphonophore tentilla are complete diverticular branchings of the tentacle ectoderm, mesoglea, and gastrovascular canal (lined by endoderm). Hessinger & Ford 1988 (in the Biology of Nematocysts) described *Physalia*'s buttons as enclosing individual fluid-filled chambers connected by narrow channels to the tentacular canal, lined by endoderm. This suggests they are not just ectodermal swellings, but probably are reduced tentilla. When we code *Physalia physalis* as tentilla bearing, the results for the character reconstruction lead to a more robust support for a tentilla-bearing MRCA followed by a single loss of tentilla in the branch leading to Apolemiidae (Supp Figure).

Siphonophore tentilla present an astounding diversity of sizes, shapes, colors, and nematocyst complements, and some have been observed to rapidly uncoil in contact with prey. Future research should explore the evolutionary history of these unique structures.

The Evolution of Vertical Habitat Use

Siphonophores are abundant predators in the pelagic realm, ranging from the surface (*Physalia physalis*) to bathypelagic depths (ref , Figure 4). While there are some pleustonic (*Physalia*) and benthic (*Rhodaliidae*) siphonophores, the phylogeny suggests the siphonophore MRCA was planktonic, as most extant taxa are. Some interesting questions arise from these facts, including 1) what was the bathymetric niche of the siphonophore MRCA, and 2) how did siphonophore's vertical habitat use of the water columns evolve along the phylogeny. Our results indicate a mesopelagic MRCA, with several convergent transition events to epipelagic and bathypelagic waters. There was only a single transition to benthic lifestyle on the stem of *Rhodaliidae*.

Discussion

The strong phylogenetic signal in the characters traditionally used for taxonomic diagnostics is a positive indicator of the applicability and unambiguity of these characters.

Conclusions

Acknowledgements

This work was supported by the National Science Foundation (DEB-1256695 and the Waterman Award). Sequencing at the Brown Genomics Core facility was supported in part by NIH P30RR031153 and NSF EPSCoR EPS-1004057. Data transfer was supported by NSF RII-C2 EPS-1005789. Analyses were conducted with computational resources and services at the Center for Computation and Visualization at Brown University, supported in part by the NSF EPSCoR EPS-1004057 and the State of Rhode Island. We also thank the MBARI crews and ROV pilots for collection of the specimens.

Supplementary Information

Agalma analysis

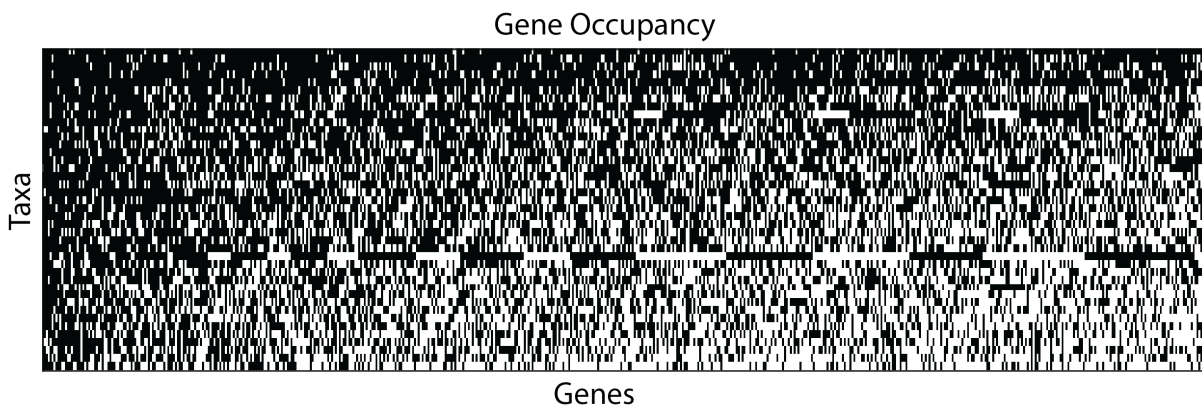


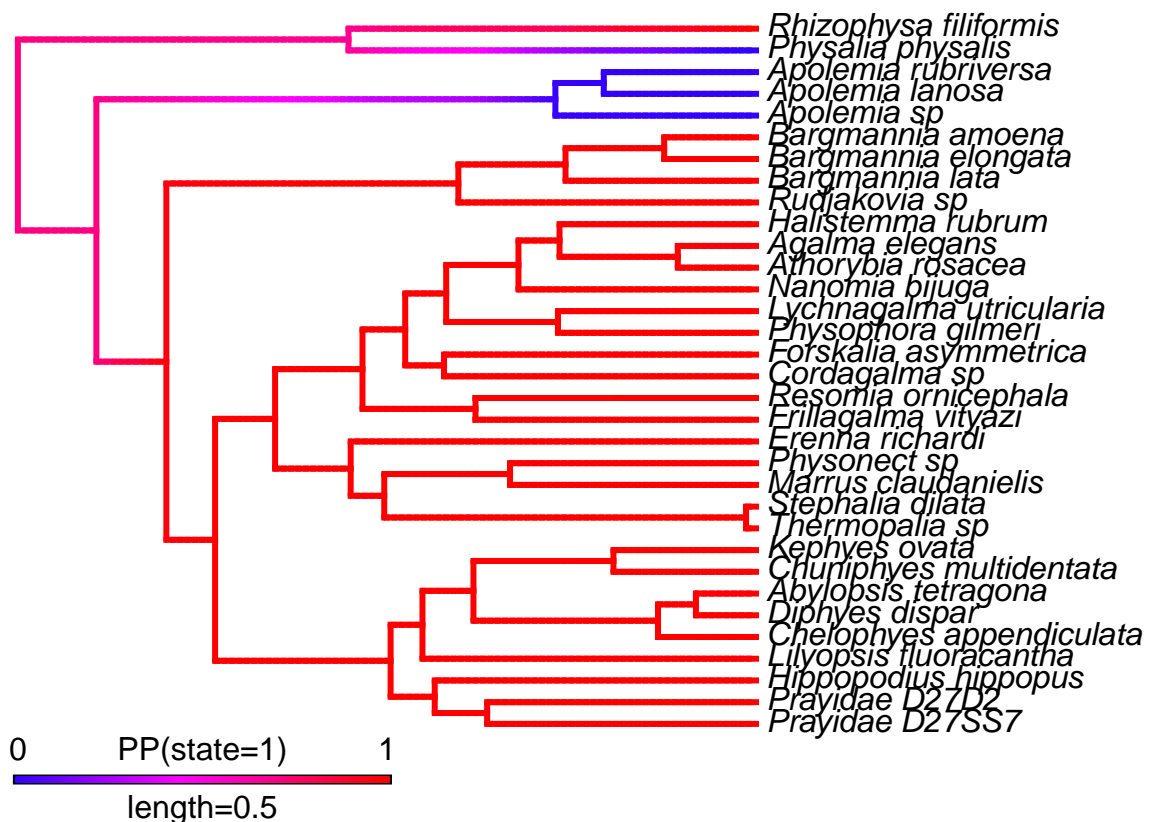
Figure 6: Supplementary Figure 1. 60% gene occupancy matrix for 41 species across 1,071 genes. Genes and species are sorted by sampling, the best sampled shown in the upper left.

Species	Mean in- sert size (bp)	Insert size sd	# pairs	% kept after rRNA re- moval	% kept after as- sem- bly	Adapter fails	Quality fails	Base Comp. fails	Total trans- cripts	Coding trans- cripts
<i>Marrus claudanielis</i>	253.03	53.30	35866092	96.80	62.10	113298	15594637	4981676	105439	22511
<i>Apolemia rubriversa</i>	290.81	80.64	19228660	91.70	77.80	40594	5179800	516100	87701	17540
<i>Chuniphyes multidentata</i>	284.46	35.74	17999147	77.00	74.30	24263	4941872	335297	84341	22084
<i>Apolemia sp</i>	167.41	53.46	16761717	81.30	79.40	1332063	3062035	41943	51470	14752
<i>Apolemia lanosa</i>	167.74	55.30	18444476	96.40	80.90	923922	3882968	439569	70184	15579
<i>Bargmannia elongata</i>	271.43	40.17	40008913	79.80	78.50	342825	8084832	2017709	152019	23661
<i>Diphyes dispar</i>	223.14	58.73	80000000	78.70	63.40	14412120	21322624	690159	210406	50868
<i>Aiptasia pallida</i>	183.18	53.88	74558341	98.40	79.30	210730	23826421	307520	83950	33523
<i>Stephalia dilata</i>	267.82	43.33	30953585	98.00	63.90	86068	15731787	1435119	107925	23984
<i>Physalia physalis</i>	233.10	54.37	36481773	96.60	88.50	18553	5491979	259497	74994	23705
<i>Bargmannia amoena</i>	161.57	53.77	20195498	84.60	80.10	1049110	3996085	274520	66726	17975
<i>Frillagalma vityazi</i>	283.11	44.91	79902051	54.00	70.40	668400	13591301	5558767	181508	29293
<i>Alatina alata</i>	173.96	60.33	96259870	52.10	77.90	1236251	15771112	468662	166584	28743
<i>Clytia hemisphaerica</i>									11476	6642
<i>Ectopleura larynx</i>	229.05	37.75	109024653	95.90	74.60	432309	40629127	897590	84034	28015
<i>Athorybia rosacea</i>	221.16	93.65	28696930	99.90	86.90	691916	4026467	633700	100839	24543
<i>Forskalia asymmetrica</i>	259.42	35.04	25275184	58.90	65.10	41922	7463840	841930	82483	18419
<i>Prayidae</i>	267.32	45.59	38233199	85.20	66.40	59773	15338562	1878732	144909	28065
<i>D27D2</i>										
<i>Lilyopsis fluoracantha</i>	259.39	39.08	51855968	76.50	65.30	72416	19809124	1388875	114662	29854
<i>Hydractinia symbiolongiplicatus</i>	175.22	57.84	60462724	49.80	85.20	162430	6678373	124392	71450	24639
<i>Rhizophysa filiformis</i>	269.74	46.52	26937827	92.50	65.30	66010	13238701	361376	110109	24833
<i>Agalma elegans</i>	238.94	57.54	40007833	99.60	86.00	31957	7177806	748977	122053	26601
<i>Chelophyes appendiculata</i>	275.93	39.43	21103284	89.00	74.20	63548	6777022	344708	110612	32309

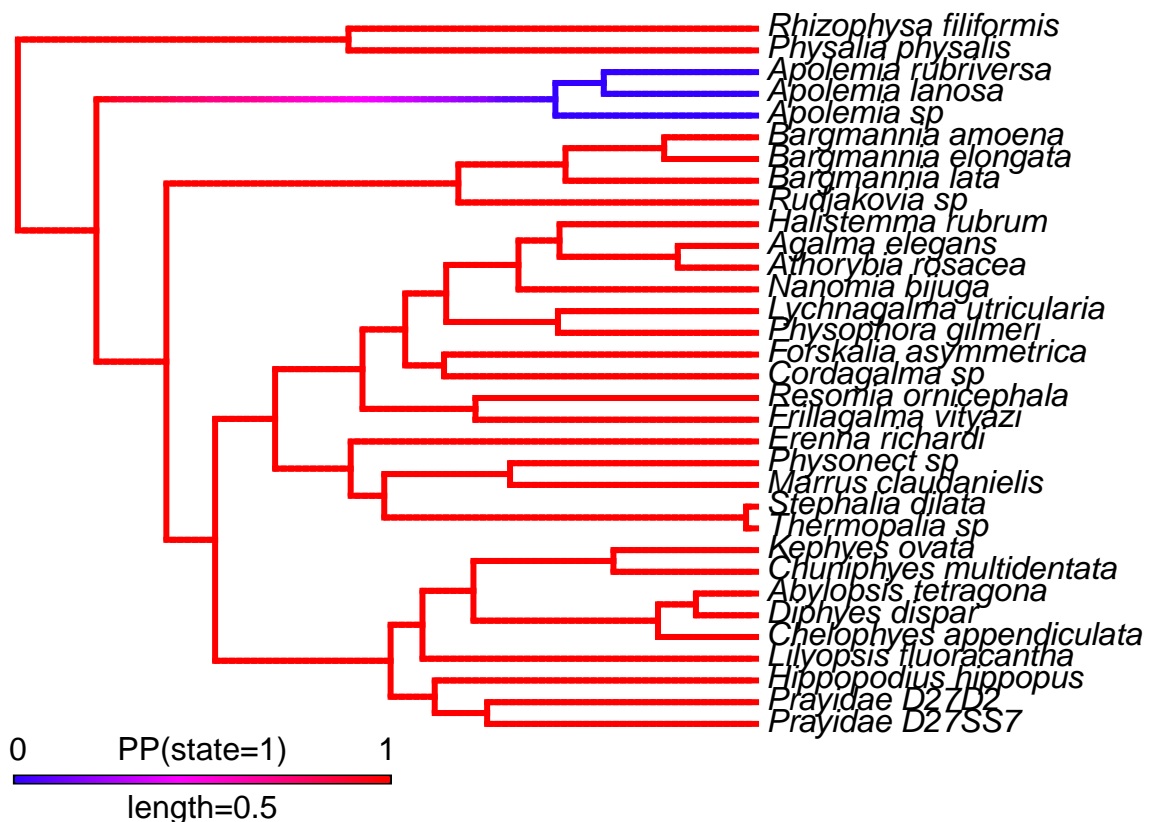
Prayidae	303.39	50.83	25233164	66.70	65.60	39061	8616289	347189	94917	24211
D27SS7										
Rudjakovia	213.88	89.71	20582477	99.10	79.70	489520	3936086	1546686	91695	24184
sp										
Abylopsis	292.16	38.32	21575176	73.30	73.80	38764	5759144	370604	102946	25268
tetragona										
Nematostella									26511	18080
vectensis										
Hippopodius	266.99	45.11	35638254	84.50	66.30	56152	15490291	535026	137341	35031
hippopus										
Physophora	214.97	93.78	19847377	99.30	81.30	936617	3464079	1007839	52639	17381
gilmeri										
Bargmannia	166.71	62.80	16984483	98.70	71.10	3118496	4227140	868584	59051	16451
lata										
Nanomia	296.69	44.20	39983229	85.70	75.50	155093	10854240	795226	165792	28927
bi-juga										
Erenna	291.53	36.76	29776547	64.20	66.60	39775	8958200	1245523	89423	18236
richardi										
Physonect	261.09	35.96	38243543	24.30	66.70	12494	4517982	274838	57746	12596
sp										
Thermopalnia	201.29	84.79	19074319	99.70	85.40	736393	2809499	531359	50572	16913
sp										
Cordagalma	289.42	37.89	20416265	62.40	77.30	22069	3875945	387383	88468	22604
sp										
Lychnagalma	266.38	50.25	35833131	63.90	65.70	60019	11691276	714049	95708	21057
utricularia										
Kephyses	243.52	61.49	42044676	99.20	85.40	12567	7982239	496206	146394	31286
ovata										
Hydra magni-papillata									17741	12581
Resomia ornicephala	258.55	36.28	42998185	68.50	65.10	47093	14776612	1429610	103682	22777
Halistemma	224.84	100.91	26331113	97.90	85.10	439185	4294857	714798	87526	25351
rubrum										
Podocoryna	173.51	52.58	46216536	72.80	74.10	121866	13195545	142954	109584	45849
carnea										

Table 2: Supplementary table 1. The assembly summary statistics for all included taxa, showing mean insert size, and the percentage of reads kept after pipeline steps.

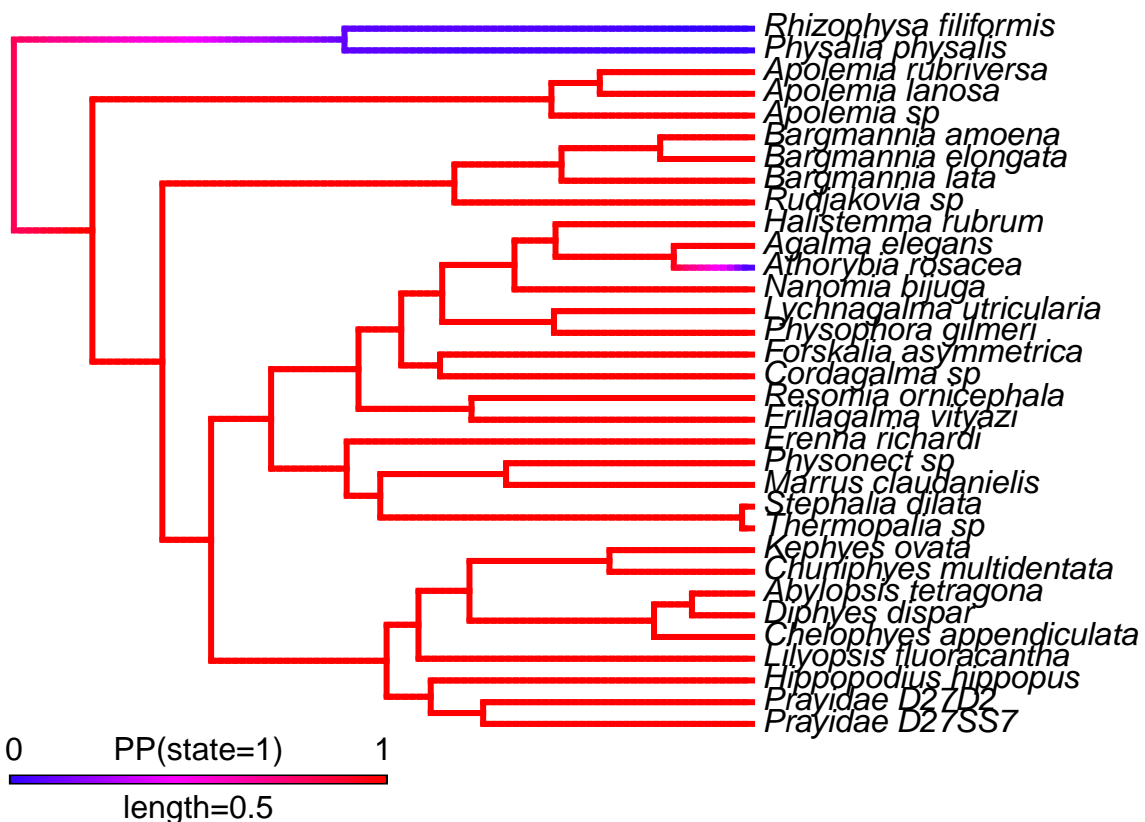
SIMMAP Presence of tentilla

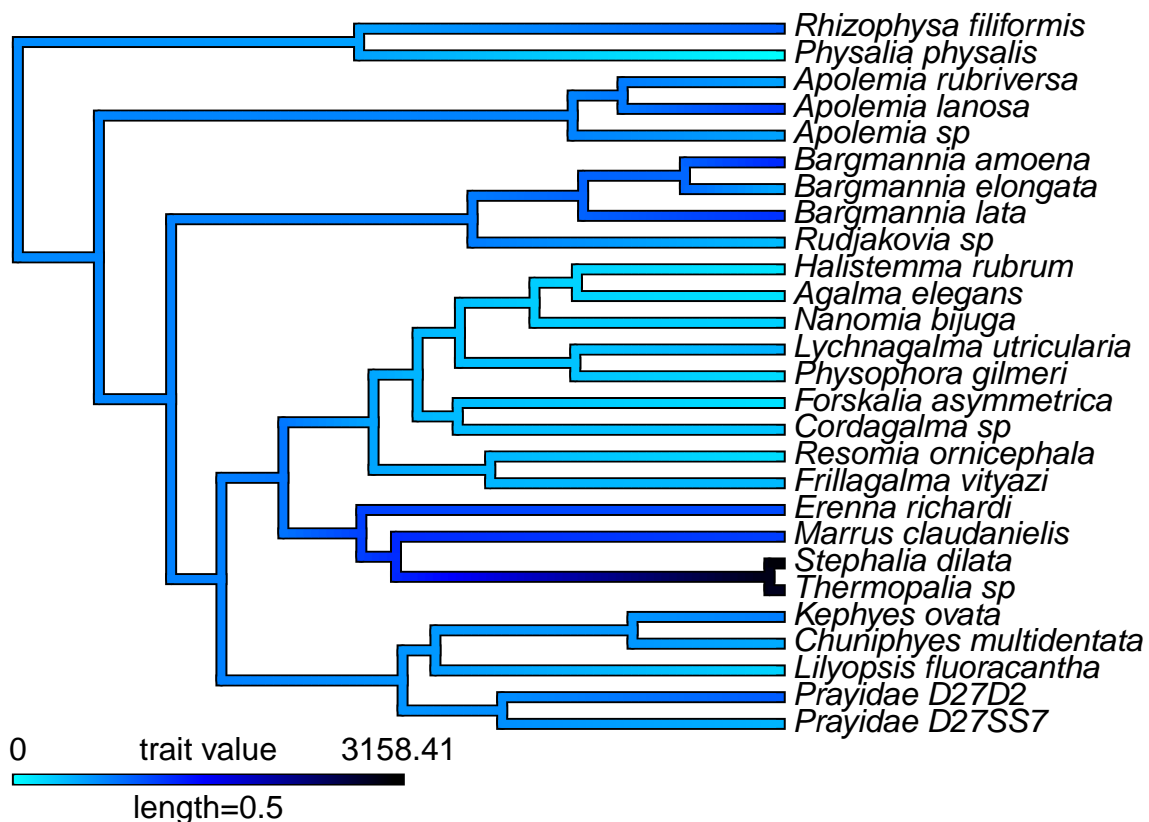


SIMMAP Presence of tentilla - *Physalia* corrected



SIMMAP Presence of Nectosome





Phylogenetic signal in Binary Traits

	K	PICvar obs	PICvar rnd	P-value	Z-score
Nectosome	0.7576294	0.20869468	0.4509368	0.2465	-0.5780613
Palpons	2.5304717	0.13420432	1.3415822	0.0010	-2.0009680
Tentilla	2.9207959	0.06470248	0.5832877	0.0010	-1.1125673
Pneumatophore	3.9935626	0.06932562	1.0900130	0.0010	-1.7502668
Bracts	1.8939556	0.08917646	0.4722604	0.0020	-0.8713691

Table 3: Supplementary table 3. Phylogenetic signal in the binary traits, including Blomberg's K statistic, the mean observed PIC variance, the random variance of PICs, p-value of the comparison of observed and random variance, and the z-score.

Software versions

This manuscript was computed on Tue Nov 28 07:56:49 PM 2017 with the following R package versions.

R version 3.4.1 (2017-06-30)

Platform: x86_64-pc-linux-gnu (64-bit)

Running under: Debian GNU/Linux 9 (stretch)

Matrix products: default

BLAS/LAPACK: /usr/lib/libopenblas-r0.2.19.so

locale:

```

[1] LC_CTYPE=en_US.UTF-8      LC_NUMERIC=C
[3] LC_TIME=en_US.UTF-8       LC_COLLATE=en_US.UTF-8
[5] LC_MONETARY=en_US.UTF-8   LC_MESSAGES=C
[7] LC_PAPER=en_US.UTF-8     LC_NAME=C
[9] LC_ADDRESS=C              LC_TELEPHONE=C
[11] LC_MEASUREMENT=en_US.UTF-8 LC_IDENTIFICATION=C

attached base packages:
[1] grid      parallel  stats      graphics  grDevices utils      datasets
[8] methods   base

other attached packages:
[1] bindrcpp_0.2    phylolm_2.5    geomorph_3.0.5   rgl_0.98.1
[5] adephylo_1.1-10 ade4_1.7-8     phylobase_0.8.4  geiger_2.0.6
[9] phangorn_2.2.0  phytools_0.6-20 picante_1.6-2   nlme_3.1-131
[13] vegan_2.4-4    lattice_0.20-35 permute_0.9-4   ape_4.1
[17] hutan_0.5.0    FactoMineR_1.38 factoextra_1.0.5 gridExtra_2.2.1
[21] seriation_1.2-2 fields_9.0     maps_3.2.0      spam_2.1-1
[25] dotCall64_0.9-04 ggtree_1.8.2   treeio_1.0.2   cowplot_0.8.0
[29] xtable_1.8-2    jsonlite_1.5   knitr_1.16     digest_0.6.12
[33] magrittr_1.5   forcats_0.2.0  stringr_1.2.0   dplyr_0.7.2
[37] purrrr_0.2.2.2  readr_1.1.1   tidyverse_1.1.1 tibble_1.3.3
[41] ggplot2_2.2.1    tidyverse_1.1.1

loaded via a namespace (and not attached):
[1] readxl_1.0.0          uuid_0.1-2
[3] backports_1.1.0        fastmatch_1.1-0
[5] plyr_1.8.4             igraph_1.1.2
[7] lazyeval_0.2.0          sp_1.2-5
[9] splines_3.4.1           rncl_0.8.2
[11] foreach_1.4.3          htmltools_0.3.6
[13] viridis_0.4.0           gdata_2.18.0
[15] cluster_2.0.6          gclus_1.3.1
[17] modelr_0.1.0           gmodels_2.16.2
[19] prettyunits_1.0.2        jpeg_0.1-8
[21] colorspace_1.3-2        rvest_0.3.2
[23] ggrepel_0.7.0           haven_1.1.0
[25] bindr_0.1                survival_2.41-3
[27] iterators_1.0.8          glue_1.1.1
[29] registry_0.3            gtable_0.2.0
[31] seqinr_3.4-5             kernlab_0.9-25
[33] prabclus_2.2-6          DEoptimR_1.0-8
[35] scales_0.4.1             mvtnorm_1.0-6
[37] Rcpp_0.12.12             plotrix_3.6-6
[39] viridisLite_0.2.0         progress_1.1.2
[41] spdep_0.6-15             flashClust_1.01-2
[43] foreign_0.8-69            subplex_1.4-1
[45] bold_0.5.0               mclust_5.3
[47] deSolve_1.20              stats4_3.4.1
[49] animation_2.5            htmlwidgets_0.9
[51] httr_1.2.1                gplots_3.0.1
[53] fpc_2.1-10               modeltools_0.2-21
[55] pkgconfig_2.0.1            reshape_0.8.7
[57] XML_3.98-1.9              flexmix_2.3-14

```

```

[59] deldir_0.1-14          nnet_7.3-12
[61] crul_0.4.0             labeling_0.3
[63] rlang_0.1.1            reshape2_1.4.2
[65] munsell_0.4.3          cellranger_1.1.0
[67] tools_3.4.1            broom_0.4.2
[69] evaluate_0.10.1         yaml_2.1.14
[71] robustbase_0.92-7       caTools_1.17.1
[73] dendextend_1.5.2        mime_0.5
[75] whisker_0.3-2          taxize_0.9.0
[77] adegenet_2.0.1          leaps_3.0
[79] xml2_1.1.1              compiler_3.4.1
[81] curl_2.8.1              clusterGeneration_1.3.4
[83] RNeXML_2.0.7             stringi_1.1.5
[85] highr_0.6                trimcluster_0.1-2
[87] Matrix_1.2-10           psych_1.7.5
[89] msm_1.6.4                LearnBayes_2.15
[91] combinat_0.0-8           data.table_1.10.4
[93] bitops_1.0-6              httpuv_1.3.5
[95] R6_2.2.2                 TSP_1.1-5
[97] KernSmooth_2.23-15       codetools_0.2-15
[99] boot_1.3-20              MASS_7.3-47
[101] gtools_3.5.0             assertthat_0.2.0
[103] rprojroot_1.2            mnormt_1.5-5
[105] diptest_0.75-7           mgcv_1.8-17
[107] expm_0.999-2             hms_0.3
[109] quadprog_1.5-5           coda_0.19-1
[111] class_7.3-14             rmarkdown_1.6
[113] rvcheck_0.0.9             shiny_1.0.3
[115] numDeriv_2016.8-1         scatterplot3d_0.3-40
[117] lubridate_1.6.0

```

References

- Beklemishev W.N., 1969. Principles of comparative anatomy of invertebrates., Edinburgh:Oliver & Boyd,
- Carré C, 1967. Le développement larvaire d'Abylopsis tetragona. Cahiers de Biologie Marine. 8, 185–193.
- Carré C., Carré D., 1991. A complete life cycle of the calycophoran siphonophore muggiae kochi (will) in the laboratory, under different temperature conditions: Ecological implications. Philosophical Transactions of the Royal Society of London B: Biological Sciences. 334, 27–32.
- Carré C., Carré D., 1995. Traité de zoologie. anatomie, systématique, biologie., Paris:Masson,
- Carré D., 1969. Etude histologique du développement de nanomia bijuga (chiaje, 1841), siphonophore physonecte, agalmidae. Cahiers de Biologie Marine. 10, 325–341.
- Cartwright P., Evans N.M., Dunn C.W., Marques A., Miglietta M.P., Schuchert P., Collins A.G., 2008. Phylogenetics of Hydrozoa (Hydrozoa: Cnidaria). Journal of the Marine Biological Association of the United Kingdom. 88, 1663.
- Cartwright P., Nawrocki A.M., 2010. Character evolution in hydrozoa (phylum cnidaria). Integrative and Comparative Biology. 50, 456–472.
- Church S.H., Ryan J.F., Dunn C.W., 2015. Automation and evaluation of the sowh test with sowhat. Systematic Biology. 64, 1048–1058.
- Dunn C., Pugh P., Haddock S., 2005. Molecular Phylogenetics of the Siphonophora (Cnidaria), with

- Implications for the Evolution of Functional Specialization. *Systematic biology*. 54, 916–935.
- Dunn C.W., Howison M., Zapata F., 2013. Agalma: an automated phylogenomics workflow. *BMC Bioinformatics*. 14, 330.
- Dunn C.W., Wagner G.P., 2006. The evolution of colony-level development in the siphonophora (cnidaria: Hydrozoa). *Development genes and evolution*. 216, 743–754.
- Huelsenbeck J.P., Nielsen R., Bollback J.P., 2003. Stochastic mapping of morphological characters. *Systematic Biology*. 52, 131–158.
- Lartillot N., Lepage T., Blanquart S., 2009. PhyloBayes 3: A bayesian software package for phylogenetic reconstruction and molecular dating. *Bioinformatics*. 25, 2286–2288.
- Lartillot N., Philippe H., 2004. A bayesian mixture model for across-site heterogeneities in the amino-acid replacement process. *Molecular Biology and Evolution*. 21, 1095–1109.
- Mackie G., Pugh P., Purcell J., 1988. Siphonophore biology. *Advances in marine biology*. 24, 97–262.
- Pagès F., González H., Ramón M., Sobarzo M., Gili J.-M., 2001. Gelatinous zooplankton assemblages associated with water masses in the humboldt current system, and potential predatory impact by bassia bassensis (siphonophora: Calycophorae). *Marine Ecology Progress Series*. 210, 13–24.
- Pugh P., 1983. Benthic siphonophores: A review of the family rhodaliidae (siphonophora, physonectae). *Philosophical Transactions of the Royal Society of London, B*. 301, 165–300.
- Pugh P., 1984. The diel migrations and distributions within a mesopelagic community in the north east atlantic. 7. siphonophores. *Progress in Oceanography*. 13, 461–489.
- Pugh P., Pages F., Boorman B., 1997. Vertical distribution and abundance of pelagic cnidarians in the eastern weddell sea, antarctica. *Journal of the marine Biological Association of the United Kingdom*. 77, 341–360.
- Purcell J., 1981. Dietary composition and diel feeding patterns of epipelagic siphonophores. *Marine Biology*. 65, 83–90.
- Revell L.J., 2012. Phytools: An r package for phylogenetic comparative biology (and other things). *Methods in Ecology and Evolution*. 3, 217–223.
- Swofford D., Olsen G., Waddell P., Hillis D., 1996. Molecular systematics. 2nd ed., Sunderland (MA): Sinauer Associates,
- Totton A., 1960. Studies on physalia physalis (l.). part 1. natural history and morphology. *Discovery Reports*. 30, 301–368.
- Totton A.K., Bargmann H.E., 1965. A synopsis of the siphonophora., British Museum (Natural History),
- Williams R., Conway D., 1981. Vertical distribution and seasonal abundance of aglantha digitale (of müller)(Coelenterata: Trachymedusae) and other planktonic coelenterates in the northeast atlantic ocean. *Journal of Plankton Research*. 3, 633–643.
- Youngbluth M.J., 1984. Water column ecology: In situ observations of marine zooplankton from a manned submersible. *Divers, submersibles and marine science*. 9, 45–57.
- Yu G., Smith D.K., Zhu H., Guan Y., Lam T.T.-Y., 2016. ggtree: an r package for visualization and annotation of phylogenetic trees with their covariates and other associated data. *Methods in Ecology and Evolution*.
- Zapata F., Goetz F.E., Smith S.A., Howison M., Siebert S., Church S.H., Sanders S.M., Ames C.L., McFadden C.S., France S.C., others, 2015. Phylogenomic analyses support traditional relationships within cnidaria. *PLoS One*. 10, e0139068.